Supplementary Information (SI) for Journal of Materials Chemistry C.

Supporting Information

Donor-Modified Tetradentate Platinum(II) Complexes for Red OLEDs

Keyue Xu,[a b] Xiaoyu Guo,[c] Jingsheng Miao,*[c] Hong Huang,[b] Nengquan Li,[b] Tao Hua,[b] Wenjing Xiong*[a] and Youming Zhang*[b]

[a] *Key Laboratory of Tropical Medicinal Resource Chemistry of Ministry of Education and Key Laboratory of Tropical Medicinal Plant Chemistry of Hainan Province, College of Chemistry and Chemical Engineering, Hainan Normal University, Haikou, Hainan, 571158, China. E-mail: xiongwj18@126.com*

[b] *Institute of Technology for Future Industry, School of Science and Technology Instrument Application Engineering, Shenzhen University of Information Technology, Shenzhen 518172, China. E-mail: zhangym@sziit.edu.cn*

[c] *College of Materials Science and Engineering, Shenzhen University, Shenzhen 518055, China. E-mail: jingshengmiao@szu.edu.cn*

Synthesis and Characterization

Unless noted, all commercial reagents were purchased and used as received without further purification. All solvents for reactions and photophysical studies were of HPLC grade. 1H nuclear magnetic resonance (NMR) spectra were recorded on a Bruker DRX 400 or JNM-ECZ600R spectrometer at 298 K. Deuterated chloroform solution was used as solvent and ^{1}H NMR spectra were recorded with tetramethyl silane (TMS) ($\delta = 0.00$ ppm) or $CDCl_3$ ($\delta = 7.26$ ppm) as internal references. High-resolution mass spectrometric measurements were performed on a Bruker Ultraflextreme spectrometer. Thermogravimetric analysis (TGA) was conducted under a dry nitrogen gas flow at a heating rate of 10 °C min^{-1} on a Netzsch STA449F5.

Photophysical Measurements

Persee TU-1950 spectrophotometer was applied to record the UV-Vis spectra. Photoluminescence (PL) spectra were recorded on a Hitachi F-7100 fluorescence spectrophotometer (Hitachi, Japan). The transient PL decay curves were obtained by FluoTime 300 spectrometer (PicoQuant GmbH) with a Picosecond Pulsed UV-LASTER (LASTER485) as the excitation source. During transient PL and PLQY measurements for thin films, the samples were exposed to dry argon to preclude the oxygen quenching effect. The photoluminescence quantum yields (PLQYs) were achieved by a Hamamatsu UV-NIR absolute PL quantum yield spectrometer (C13534, Hamamatsu Photonics) equipped with a calibrated integrating sphere. Thin doped PMMA and neat films for steady state and transient photoluminescence measurements were prepared by drop-casting of a solution followed by air-drying.

X-ray Crystallography

Single crystals of all complexes were obtained by layering methanol onto a DCM solution of each complex which undergoes slow diffusion. X-ray diffractions of all complexes were recorded on a XtaLAB AFC12 (RINC): Kappa single diffractometer (Rigaku, Japan) with Cu Kα radiation (λ = 1.54184 Å). The crystal was kept at 298 K during data collection. Using Olex2[1], the structure was determined with the ShelXT[2] structure solution program using intrinsic phasing and refined with the ShelXL refinement package using least-squares minimization[3]. Full crystallographic information in CIF format has been deposited at the Cambridge Crystallographic Data Center (CCDC), which can be obtained free from the website of www.ccdc.cam.ac.un/conts/retrieving.html.

Quantum chemical calculations

Quantum chemical calculations were performed using the Gaussian 09 program package[4], using the B3LYP functional[5], LANL2DZ[6] basis set for platinum, and 6-31G for all other atoms[7]. The dichloromethane was applied as solvent to FMOs and T_1 calculations. No solvent was applied to others calculations, and results were analyzed further with Gauss View. Time-dependent DFT (TD-DFT) calculations were also carried out by this method on the basis of optimized ground-state geometries. The RMSDs were calculated with the software of VMD by referring to the configuration of S_0. The SOCs between S_n (n = 0, 1, 1) and T_n (n = 1, 2) states were calculated with PySOC by considering that the three T_n substrates (m = 1, 0, -1) are degenerate, i.e., $\left\langle S_n \middle| \hat{H}_{so} \middle| T_n^m \right\rangle = \sqrt{\sum_{m=0,\pm 1} \left\langle S_n \middle| \hat{H}_{so} \middle| T_n^m \right\rangle^2}$. All SOCs were obtained at the TD-DFT level of theory using the B3LYP functional and the 6-31G(d) basis

set. The root-mean-square displacements (RMSD) between T_1 and S_0 states were calculated with Visual Molecular Dynamics (VMD) program by using the Cartesian coordinates of complexes at the optimized S_0 and T_1 geometry, i.e., RMSD = $\sqrt{\frac{1}{N}\sum_{i}^{natom}\left[\left[x_i - x_i^{'}\right]^2 + \left(y_i - y_i^{'}\right)^2 + \left(z_i - z_i^{'}\right)^2\right]}$, Where N is the total number of atoms, x, y, and z represent the Cartesian coordinates of each atom.

Device fabrication and characterization

For devices fabrications, the layers of ITO/HAT-CN (5 nm)/TAPC (30 nm)/TCTA (15 nm)/DMIC-TRz: Pt(II) emitter (45 nm)/Na-An-Bl (40 nm)/Liq (2 nm)/Al (100 nm) were successively deposited on the pre-cleaned ITO glass substrates at a pressure of less than 10^{-4} Pa. Indium-tin-oxide (ITO) coated glass with a sheet resistance of 10 Ω/sq was used as the anode substrate. Before film deposition, patterned ITO substrates were cleaned with detergent, rinsed in de-ionized water, acetone, and isopropanol, and then dried in an oven for 1 h in a cleanroom. The slides were then treated in an ultraviolet-ozone chamber for 5 min. The active area of devices was 3 mm × 3 mm. The EL spectra of devices were measured by fiber optic spectrometer (Ocean Optics USB 2000) in the normal direction. The *J-V-L* curves were investigated by a dual-channel Keithley 2614B source measure unit and a PIN-25D silicon photodiode. All the measurements were conducted at room temperature under ambient condition. For operational stability studies, the devices were encapsulated with glass lids by UV curing adhesive in a nitrogen-filled glove box and then taken out from the glove box for lifetime tests. The luminance of the working devices in the normal direction were measured using an OLED lifetime testing system (FS-MP64, Suzhou FSTAR Scientific

Instrument Co., Ltd, China) under a constant current density.

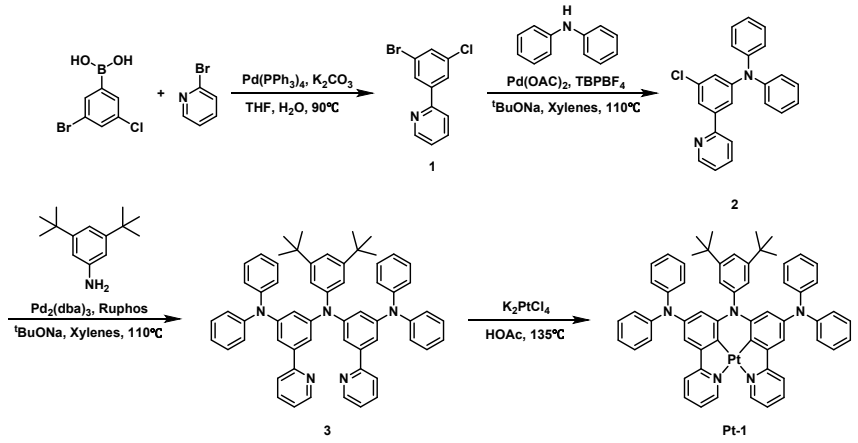

Scheme S1. Synthetic routes for **Pt-1**.

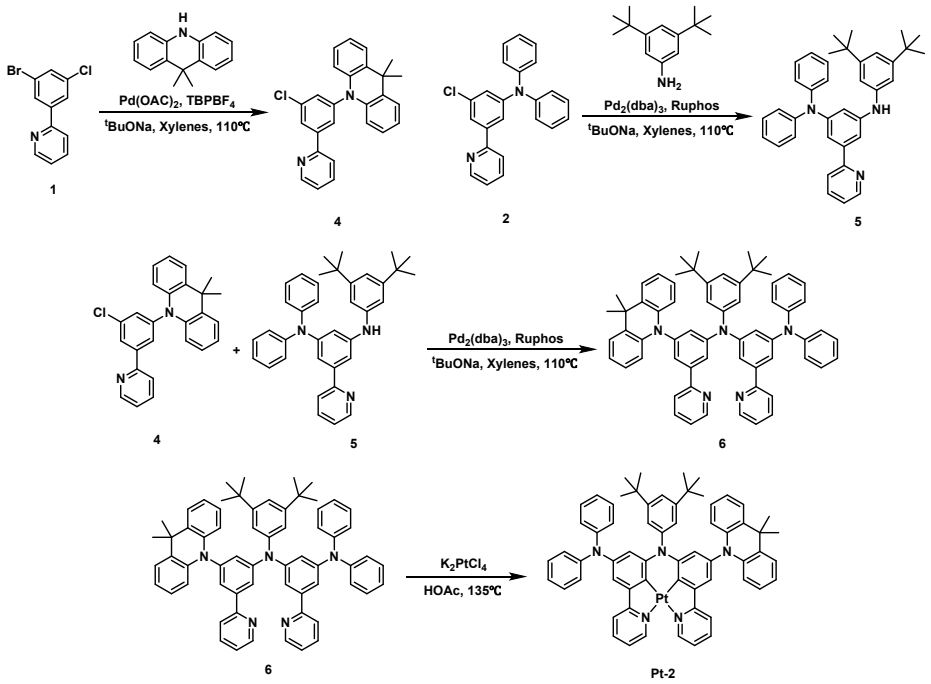

Scheme S2. Synthetic routes for **Pt-2**.

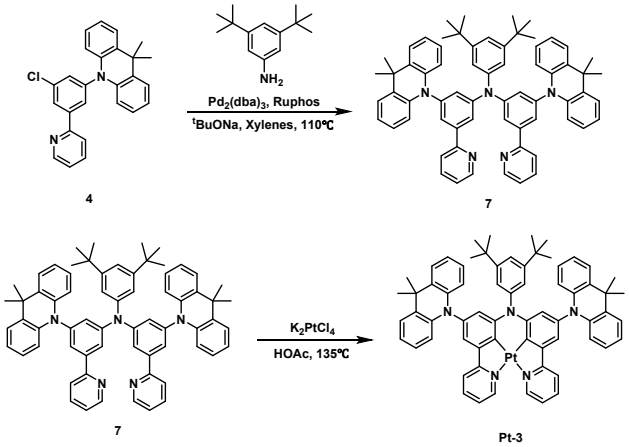

Scheme S3. Synthetic routes for **Pt-3**.

Synthesis of 2-(3-bromo-5-chlorophenyl)pyridine (**1**): A mixture of (3-bromo-5-chlorophenyl)boronic acid (10 g, 42.5 mmol), 2-bromopyridine (6.86 g, 42.5 mmol), and $Pd(PPh_3)_4$ (500 mg, 0.43 mmol) was added to a degassed mixture of tetrahydrofuran (80mL) and 2 mol/L potassium carbonate aqueous solution (20 mL). The mixture was refluxed for 24 h under the protection of nitrogen. After being cooled to room temperature, the mixture was poured into water (50 mL). It was extracted with dichloromethane (DCM) (3 × 100 mL) and the combined organic layer was dried over anhydrous magnesium sulfate. The solvent was removed off by rotary evaporation and the residue was passed through a flash silica gel column with petroleum ether (PE)/dichloromethane (DCM) as the eluent to give a faint yellow solid (5.6 g, yield 52%). ^{1}H NMR (600 MHz, Chloroform-d) δ 8.70 (s, 1H), 8.05 (d, J = 3.9 Hz, 1H), 7.94 (s, 1H), 7.79 (s, 1H), 7.69 (d, J = 8.6 Hz, 1H), 7.56 (s, 1H), 7.32 – 7.28 (m, 1H).

Synthesis of 3-chloro-N,N-diphenyl-5-(pyridin-2-yl)aniline (**2**): To a mixture of **compound 1** (1 g, 3.7 mmol), diphenylamine (0.63 g, 3.7 mmol), palladium acetate (84 mg, 0.4 mmol), tri-*tert*-butylphosphine tetrafluoroborate (216 mg, 0.7 mmol) and sodium *tert*-butoxide (1.07 g, 11.2 mmol) was added a degassed mixture of xylene (40 mL). The mixture was refluxed for 5 h under the protection of nitrogen. After being cooled to room temperature, the mixture was poured into water (50 mL). It was extracted with DCM (3 × 50 mL) and the combined organic layer was dried over anhydrous magnesium sulfate. The solvent was removed off by rotary evaporation and the residue was passed through a flash silica gel column with PE/DCM as the eluent to give a yellow solid (0.77 g, yield 57%). ^{1}H NMR (600 MHz, Chloroform-*d*)

δ 8.63 (ddd, J = 4.8, 1.9, 0.9 Hz, 1H), 7.70 (td, J = 7.7, 1.8 Hz, 1H), 7.59 (t, J = 1.7 Hz, 1H), 7.56 – 7.54 (m, 2H), 7.31 – 7.26 (m, 4H), 7.22 (ddd, J = 7.5, 4.8, 1.1 Hz, 1H), 7.14 – 7.12 (m, 4H), 7.09 – 7.05 (m, 3H).

Synthesis of N^1-(3,5-di-tert-butylphenyl)-N^1-(3-(diphenylamino)-5-(pyridin-2-yl)phenyl)-N^3,N^3-diphenyl-5-(pyridin-2-yl)benzene-1,3-diamine (**3**): To a mixture of **compound 2** (1 g, 2.8 mmol), 3,5-di-tert-butylaniline (288 mg, 1.4 mmol), $Pd_2(dba)_3$ (257 mg, 0.3 mmol), Ruphos (262 mg, 0.6 mmol) and sodium *tert*-butoxide (810 mg, 8.4 mmol) was added a degassed mixture of xylene (50 mL). The mixture was refluxed for 24 h under the protection of nitrogen. After being cooled to room temperature, the mixture was poured into water (50 mL). It was extracted with DCM (3 × 50 mL) and the combined organic layer was dried over anhydrous magnesium sulfate. The solvent was removed off by rotary evaporation and the residue was passed through a flash silica gel column with petroleum ether (PE)/ ethyl acetate (EA) as the eluent to give a white solid (1.062 g, yield 89%). ^{1}H NMR (600 MHz, Chloroform-*d*) δ 8.59 (ddd, J = 4.9, 1.9, 0.9 Hz, 2H), 7.65 (td, J = 7.7, 1.8 Hz, 2H), 7.48 (dt, J = 8.1, 1.1 Hz, 2H), 7.41 (t, J = 1.8 Hz, 2H), 7.31 (t, J = 1.8 Hz, 2H), 7.17 (ddd, J = 7.5, 4.8, 1.1 Hz, 2H), 7.14 – 7.11 (m, 8H), 7.05 – 7.01 (m, 9H), 6.96 (d, J = 1.7 Hz, 2H), 6.92 (tt, J = 7.5, 1.2 Hz, 4H), 6.87 (t, J = 2.1 Hz, 2H), 1.21 (s, 18H).

*Synthesis of **Pt-1***: **Compound 3** (527 mg, 0.6 mmol), K_2PtCl_4 (310 mg, 0.7 mmol) were added to a three-necked flask equipped with a magnetic stir bar. The flask then underwent a procedure of evacuation and backfill with nitrogen three times. A solvent of acetic acid

(HOAc) (50 ml) was added under nitrogen. The mixture was stirred in an oil bath under reflux for 5 h, then cooled to ambient temperature. The mixture was added to water. The resulting precipitate was filtered and washed with water and methanol. The filter residue was passed through a flash silica gel column with PE/DCM as the eluent to obtain desired product **Pt-1** as a red solid (yield: 277 mg, 43%). ^{1}H NMR (600 MHz, Chloroform-*d*) δ 8.97 – 8.92 (m, 2H), 7.84 – 7.76 (m, 4H), 7.35 (ddd, J = 7.2, 5.6, 1.6 Hz, 2H), 7.18 (d, J = 1.9 Hz, 2H), 7.14 – 7.05 (m, 9H), 6.98 – 6.92 (m, 8H), 6.89 – 6.80 (m, 6H), 6.11 (d, J = 1.8 Hz, 2H), 1.06 (s, 18H). MALDI-TOF-MS (m/z) calcd for $C_{60}H_{53}N_5Pt$ $[M]^+$, 1038.3949; found, 1038.3945.

Synthesis of 10-(3-chloro-5-(pyridin-2-yl)phenyl)-9,9-dimethyl-9,10-dihydroacridine (**4**): To a mixture of **compound 1** (1 g, 3.7 mmol), 9,9-dimethyl-9,10-dihydroacridine (779 mg, 3.7 mmol), palladium acetate (84 mg, 0.4 mmol), tri-*tert*-butylphosphine tetrafluoroborate (216 mg, 0.7 mmol) and sodium *tert*-butoxide (1.07 g, 11.2 mmol) was added a degassed mixture of xylene (50 mL). The mixture was refluxed for 5 h under the protection of nitrogen. After being cooled to room temperature, the mixture was poured into water (50 mL). It was extracted with DCM (3 × 50 mL) and the combined organic layer was dried over anhydrous magnesium sulfate. The solvent was removed off by rotary evaporation and the residue was passed through a flash silica gel column with PE/DCM as the eluent to give a yellow solid (665 mg, yield 43%). ^{1}H NMR (600 MHz, Chloroform-*d*) δ 8.71 (ddd, J = 4.8, 1.8, 0.9 Hz, 1H), 8.24 (t, J = 1.8 Hz, 1H), 7.88 (t, J = 1.7 Hz, 1H), 7.82 – 7.69 (m, 2H), 7.47 (dd, J = 7.7, 1.6 Hz, 2H), 7.42 (t, J = 1.9 Hz, 1H), 7.29 (ddd, J = 7.3, 4.8, 1.3 Hz, 1H), 6.97 (dtd, J = 27.6, 7.2, 1.5 Hz, 4H), 6.36 (dd, J = 8.1, 1.3 Hz, 2H), 1.71 (s, 6H).

Synthesis of N^1-(3,5-di-tert-butylphenyl)-N^3,N^3-diphenyl-5-(pyridin-2-yl)benzene-1,3-diamine (**5**): To a mixture of **compound 2** (1 g, 2.0 mmol), 3,5-di-tert-butylaniline (419 mg, 2.0 mmol), $Pd_2(dba)_3$ (187 mg, 0.2 mmol), Ruphos (191 mg, 0.4 mmol) and sodium *tert*-butoxide (810 mg, 8.4 mmol) was added a degassed mixture of xylene (50 mL). The mixture was refluxed for 24 h under the protection of nitrogen. After being cooled to room temperature, the mixture was poured into water (50 mL). It was extracted with DCM (3 × 50 mL) and the combined organic layer was dried over anhydrous magnesium sulfate. The solvent was removed off by rotary evaporation and the residue was passed through a flash silica gel column with PE/EA as the eluent to give a white solid (685 mg, yield 64%). ^{1}H NMR (600 MHz, Chloroform-*d*) δ 8.61 (ddd, J = 4.8, 1.8, 0.9 Hz, 1H), 7.67 (td, J = 7.7, 1.9 Hz, 1H), 7.56 (dt, J = 8.0, 1.1 Hz, 1H), 7.38 (dd, J = 2.2, 1.5 Hz, 1H), 7.25 – 7.21 (m, 5H), 7.18 (ddd, J = 7.5, 4.8, 1.1 Hz, 1H), 7.15 – 7.12 (m, 4H), 7.00 – 6.97 (m, 3H), 6.90 (d, J = 1.7 Hz, 2H), 6.88 (t, J = 2.1 Hz, 1H), 5.80 (s, 1H), 1.25 (s, 18H).

Synthesis of N^1-(3,5-di-tert-butylphenyl)-N^1-(3-(9,9-dimethylacridin-10(9H)-yl)-5-(pyridin-2-yl)phenyl)-N^3,N^3-diphenyl-5-(pyridin-2-yl)benzene-1,3-diamine (**6**): To a mixture of **compound 4** (568 mg, 1.4 mmol), **compound 5** (685 mg, 1.3 mmol), $Pd_2(dba)_3$ (119 mg, 0.1 mmol), Ruphos (122 mg, 0.3 mmol) and sodium *tert*-butoxide (376 mg, 3.9 mmol) was added a degassed mixture of xylene (30 mL). The mixture was refluxed for 24 h under the protection of nitrogen. After being cooled to room temperature, the mixture was poured into water (30 mL). It was extracted with DCM (3 × 50 mL) and the combined organic layer was dried over

anhydrous magnesium sulfate. The solvent was removed off by rotary evaporation and the residue was passed through a flash silica gel column with PE/EA as the eluent to give a white solid (775 mg, yield 70%). ^{1}H NMR (600 MHz, Chloroform-*d*) δ 8.67 (dd, J = 4.5, 1.5 Hz, 1H), 8.59 (d, J = 4.8 Hz, 1H), 7.96 (t, J = 1.9 Hz, 1H), 7.78 – 7.61 (m, 3H), 7.57 – 7.34 (m, 6H), 7.25 – 7.21 (m, 1H), 7.21 – 7.15 (m, 1H), 7.12 – 7.03 (m, 12H), 6.95 – 6.85 (m, 7H), 6.41 – 6.33 (m, 2H), 1.65 (s, 6H), 1.21 (s, 18H).

Synthesis of ***Pt-2***: **Compound 6** (775 mg, 0.9 mmol), K_2PtCl_4 (436 mg, 1.1 mmol) were added to a three-necked flask equipped with a magnetic stir bar. The flask then underwent a procedure of evacuation and backfill with nitrogen three times. A solvent of acetic acid (HOAc) (50 ml) was added under nitrogen. The mixture was stirred in an oil bath under reflux for 5 h, then cooled to ambient temperature. The mixture was added to water. The resulting precipitate was filtered and washed with water and methanol. The filter residue was passed through a flash silica gel column with PE/DCM as the eluent to obtain desired product **Pt-2** as a red solid (yield: 426 mg, 45%). ^{1}H NMR (600 MHz, Chloroform-*d*) δ 8.97 (t, J = 6.6 Hz, 2H), 7.89 – 7.79 (m, 4H), 7.44 – 7.33 (m, 4H), 7.23 (dd, J = 8.7, 1.8 Hz, 2H), 7.16 – 7.07 (m, 5H), 7.03 (d, J = 1.7 Hz, 2H), 7.01 – 6.95 (m, 4H), 6.91 – 6.80 (m, 6H), 6.49 (dd, J = 8.1, 1.4 Hz, 2H), 6.32 – 6.16 (m, 2H), 1.60 (s, 6H), 1.06 (s, 18H). MALDI-TOF-MS (m/z) calcd for $C_{63}H_{57}N_5Pt$ $[M]^+$, 1078.4262; found, 1078.4256.

Synthesis of 3,5-di-tert-butyl-N,N-bis(3-(9,9-dimethylacridin-10(9H)-yl)-5-(pyridin-2-yl)phenyl)aniline (**7**): To a mixture of **compound 4** (1.5 g, 3.8 mmol), 3,5-di-tert-butylaniline

(310 mg, 1.5 mmol), $Pd_2(dba)_3$ (346 mg, 0.4 mmol), Ruphos (353 mg, 0.8 mmol) and sodium *tert*-butoxide (1.09 g, 11.3 mmol) was added a degassed mixture of xylene (50 mL). The mixture was refluxed for 24 h under the protection of nitrogen. After being cooled to room temperature, the mixture was poured into water (50 mL). It was extracted with DCM (3 × 50 mL) and the combined organic layer was dried over anhydrous magnesium sulfate. The solvent was removed off by rotary evaporation and the residue was passed through a flash silica gel column with PE/EA as the eluent to give a white solid (762 mg, yield 54%). ^{1}H NMR (600 MHz, Chloroform-*d*) δ 8.65 – 8.61 (m, 2H), 8.11 – 8.03 (m, 3H), 7.72 – 7.66 (m, 2H), 7.61 (d, J = 8.0 Hz, 2H), 7.57 (t, J = 1.7 Hz, 2H), 7.39 (dd, J = 7.4, 1.9 Hz, 4H), 7.21 (tt, J = 3.7, 2.0 Hz, 4H), 7.11 (s, 2H), 6.87 (dtd, J = 16.5, 7.2, 1.6 Hz, 8H), 6.46 (dd, J = 7.8, 1.6 Hz, 4H), 1.64 (s, 12H), 1.18 (s, 18H).

Synthesis of ***Pt-3***: **Compound 7** (760 mg, 0.8 mmol), K_2PtCl_4 (409 mg, 1.0 mmol) were added to a three-necked flask equipped with a magnetic stir bar. The flask then underwent a procedure of evacuation and backfill with nitrogen three times. A solvent of acetic acid (HOAc) (50 ml) was added under nitrogen. The mixture was stirred in an oil bath under reflux for 5 h, then cooled to ambient temperature. The mixture was added to water. The resulting precipitate was filtered and washed with water and methanol. The filter residue was passed through a flash silica gel column with PE/DCM as the eluent to obtain desired product **Pt-3** as a red solid (yield: 412 mg, 46%). ^{1}H NMR (600 MHz, Chloroform-*d*) δ 9.00 (d, J = 5.6 Hz, 2H), 7.93 – 7.88 (m, 4H), 7.45 (q, J = 5.0 Hz, 2H), 7.37 (dd, J = 7.6, 1.6 Hz, 4H), 7.29 (d, J = 1.7 Hz, 2H), 7.20 – 7.13 (m, 3H), 6.87 (dtd, J = 26.2, 7.3, 1.5 Hz, 8H), 6.52 (dd, J =

8.2, 1.4 Hz, 4H), 6.36 (d, J = 1.8 Hz, 2H), 1.61 (s, 12H), 1.04 (s, 18H). MALDI-TOF-MS (m/z) calcd for $C_{66}H_{61}N_5Pt$ $[M]^+$, 1118.4575; found, 1118.4557.

Table S1. Crystal data and structure refinement for complexes **Pt-1** and **Pt-3**

Identification code	**Pt-1**	**Pt-3**
Empirical formula	$C_{60}H_{53}N_5Pt \cdot CH_2Cl_2$	$C_{66}H_{61}N_5Pt \cdot 2(CH_2Cl_2)$
Formula weight	1124.09	1289.14
Temperature/K	298.38(10)	200.06(11)
Crystal system	triclinic	monoclinic
Space group	P-1	$P2_1/c$
a/Å	9.5741(2)	20.6396(4)
b/Å	14.3170(4)	11.7535(2)
c/Å	20.4183(3)	24.6159(4)
α/°	88.7087(17)	90
β/°	81.2010(17)	98.9595(16)
γ/°	71.071(2)	90
Volume/Å^3	2615.16(11)	5898.63(18)
Z	2	4
ρ_{calc}g/cm^3	1.428	1.452
μ/mm^{-1}	6.291	6.468
F(000)	1136.0	2616.0
Crystal size/mm^3	0.14 × 0.1 × 0.08	0.14 × 0.12 × 0.11
Radiation	Cu Kα (λ = 1.54184)	Cu Kα (λ = 1.54184)
2Θ range for data collection/°	7.76 to 146.122	4.334 to 149.84
Reflections collected	41712	35540
Independent reflections	9868 [R_{int} = 0.0331, R_{sigma} = 0.0260]	11603 [R_{int} = 0.0372, R_{sigma} = 0.0372]
Data/restraints/parameters	9868/0/659	11603/0/713
Goodness-of-fit on F^2	1.014	1.021
Final R indexes [I>=2σ (I)]	R_1 = 0.0253, wR_2 = 0.0611	R_1 = 0.0379, wR_2 = 0.1002
Final R indexes [all data]	R_1 = 0.0294, wR_2 = 0.0629	R_1 = 0.0528, wR_2 = 0.1157
Largest diff. peak/hole / e Å^{-3}	0.67/-0.71	1.25/-1.33
CCDC No.	2452972	2452980

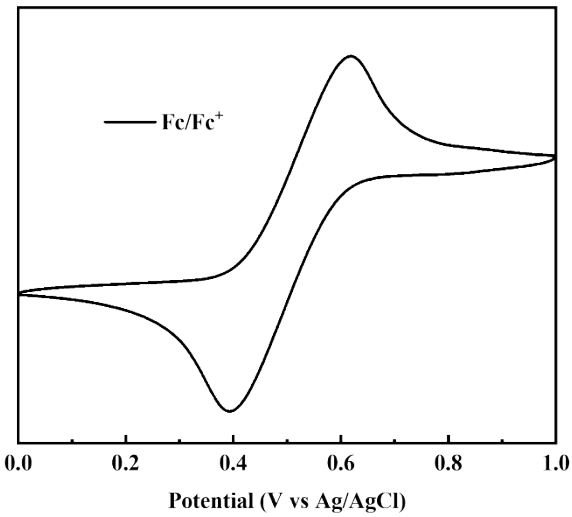

Figure S1. Cyclic voltammograms of ferrocene in DCM solution with a scan rate of 100 mV s^{-1} using 0.1 mol/L Bu_4NPF_6.

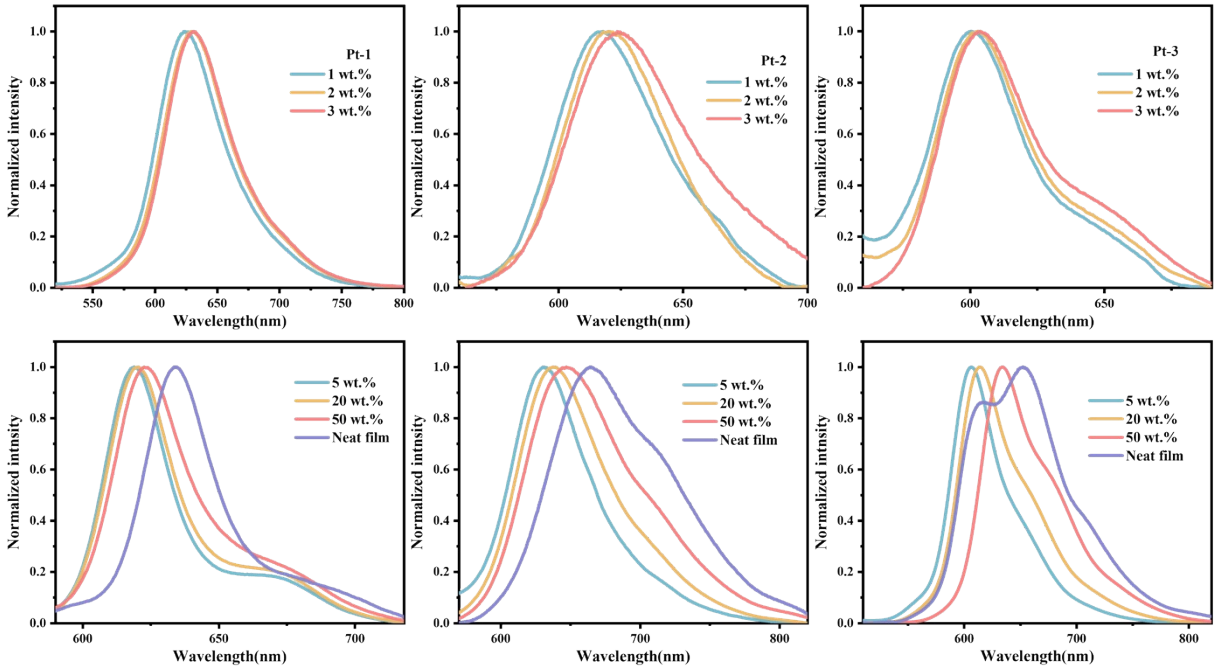

Figure S2. PL spectra of **Pt-1** to **Pt-3** in PMMA at various concentrations (1-3 wt.% ,5 wt.%, 20 wt.%, and 50 wt.%) and in neat film.

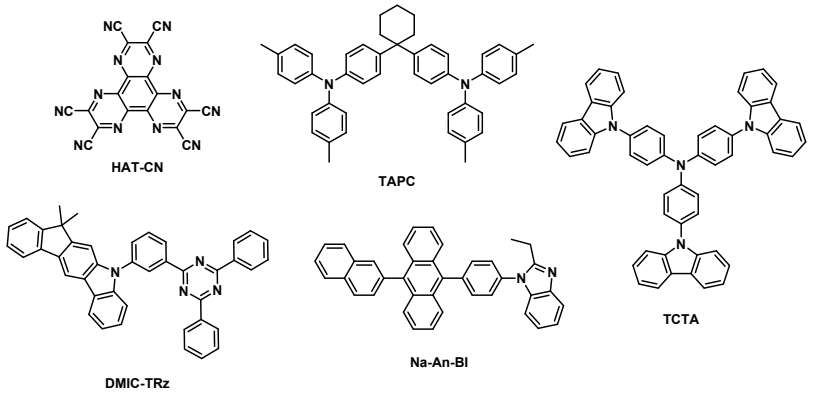

Figure S3. Chemical structures of HAT-CN, TAPC, TCTA, DMIC-TRz and Na-An-BI.

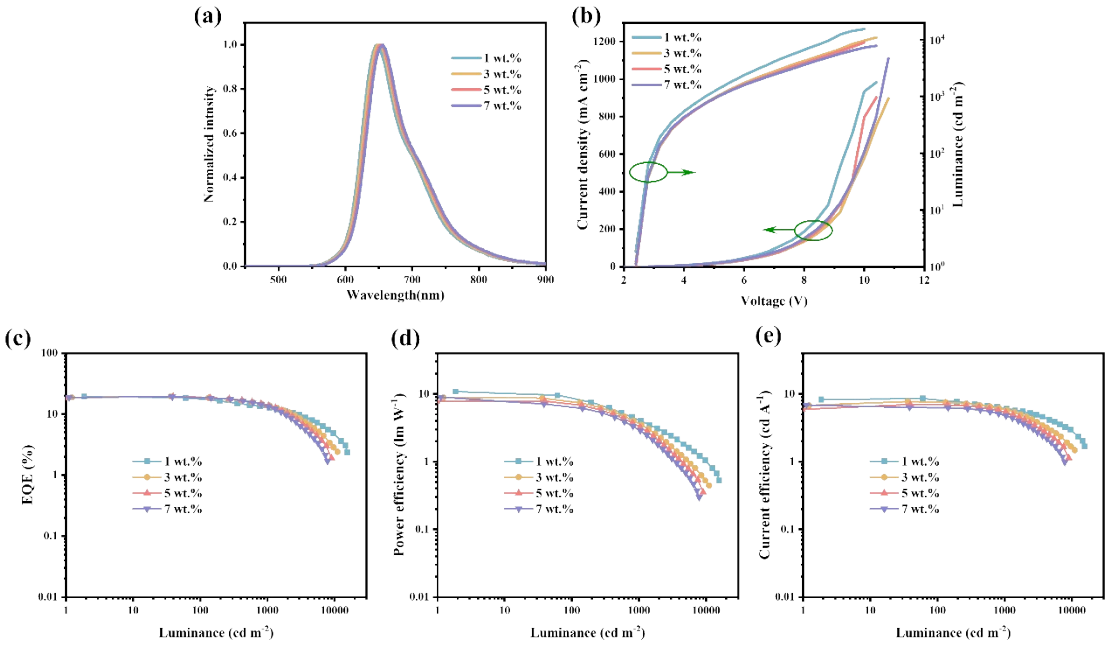

Figure S4. (a) Normalized EL spectra, (b) current density-voltage-luminance characteristics, (c) EQE-luminance characteristics, (d) PE-luminance characteristics, (e) CE-luminance characteristics of OLEDs with **Pt-1** as the emitter.

Table S2. Key performances of OLEDs based on **Pt-1** as the emitter.

Pt-1	**λ (nm)**	L^a_{max} (cd m^{-2})	CE^b (cd A^{-1})	PE^c (lm W^{-1})	EQE^d (%)	CIE^e (x, y)
1 wt.%	648	15578	8.3/6.1	10.8/4.0	19.5/12.6	0.70, 0.31
3 wt.%	650	11075	7.7/5.8	8.7/3.5	19.5/13.7	0.69, 0.31
5 wt.%	652	9020	7.0/5.3	7.8/3.2	19.4/13.9	0.70, 0.30
7 wt.%	655	7892	6.3/4.7	7.1/2.9	19.2/13.3	0.70, 0.30

(a) Maximum luminance. (b) The maximum current efficiency (left) and the value at 1000 cd m^{-2} (right). (c) The maximum power efficiency (left) and the value at 1000 cd m^{-2} (right). (d) The maximum external quantum efficiency (left) and the value at 1000 cd m^{-2} (right). (e) CIE coordinates @EQE_{max}.

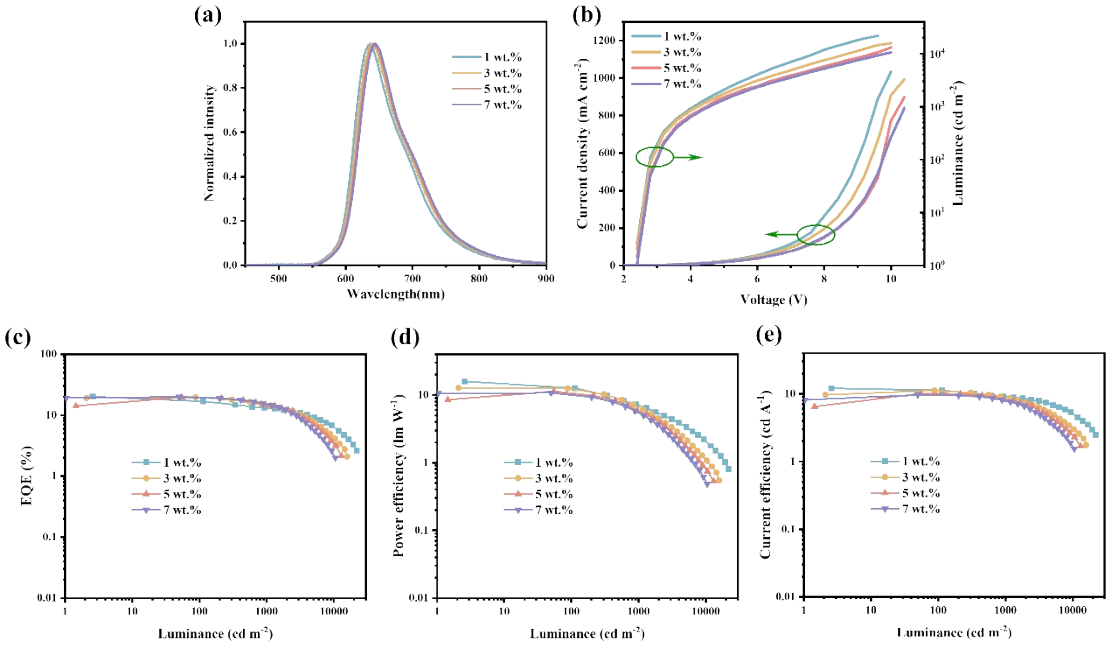

Figure S5. (a) Normalized EL spectra, (b) current density-voltage-luminance characteristics, (c) EQE-luminance characteristics, (d) PE-luminance characteristics, (e) CE-luminance characteristics of OLEDs with **Pt-2** as the emitter.

Table S3. Key performances of OLEDs based on **Pt-2** as the emitter.

Pt-2	**λ (nm)**	L^a_{max} (cd m^{-2})	*CE*^{b} (cd A^{-1})	*PE*^{c} (lm W^{-1})	*EQE*^{d} (%)	*CIE*^{e} (x, y)
1 wt.%	636	21973	12.1/9.3	15.8/7.3	20.1/13.3	0.69, 0.32
3 wt.%	640	15874	11.2/8.6	12.5/6.1	19.8/14.3	0.68, 0.32
5 wt.%	643	13075	10.1/8.2	11.3/5.8	19.7/14.9	0.69, 0.31
7 wt.%	645	10548	9.6/8.1	10.7/5.8	19.9/15.7	0.69, 0.31

(a) Maximum luminance. (b) The maximum current efficiency (left) and the value at 1000 cd m^{-2} (right). (c) The maximum power efficiency (left) and the value at 1000 cd m^{-2} (right). (d) The maximum external quantum efficiency (left) and the value at 1000 cd m^{-2} (right). (e) CIE coordinates @EQE$_{max}$.

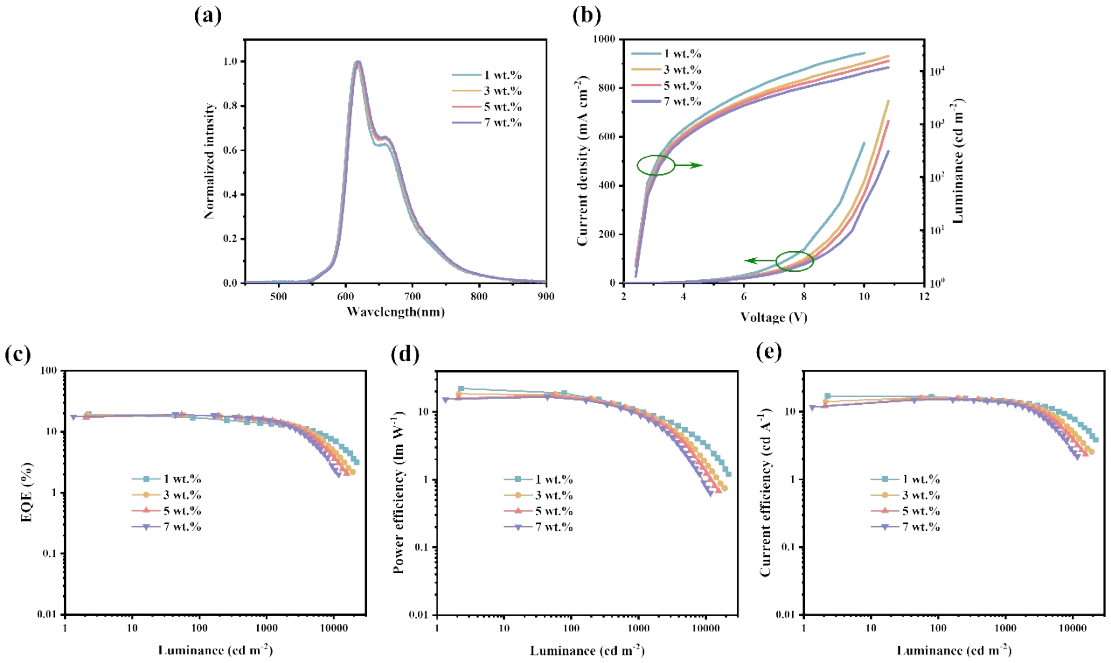

Figure S6. (a) Normalized EL spectra, (b) current density-voltage-luminance characteristics, (c) EQE-luminance characteristics, (d) PE-luminance characteristics, (e) CE-luminance characteristics of OLEDs with **Pt-3** as the emitter.

Table S4. Key performances of OLEDs based on **Pt-3** as the emitter.

Pt-3	**λ (nm)**	L^a_{max} (cd m^{-2})	*CE*^{b} (cd A^{-1})	*PE*^{c} (lm W^{-1})	*EQE*^{d} (%)	*CIE*^{e} (x, y)
1 wt.%	616	21927	17.0/13.9	22.2/9.9	19.2/13.4	0.66, 0.34
3 wt.%	617	19184	16.1/14.4	18.4/10.3	18.8/15.5	0.67, 0.33
5 wt.%	619	15535	15.5/14.3	17.4/10.2	19.0/16.0	0.67, 0.33
7 wt.%	620	11777	15.0/13.4	16.6/8.8	19.0/15.4	0.67, 0.33

(a) Maximum luminance. (b) The maximum current efficiency (left) and the value at 1000 cd m^{-2} (right). (c) The maximum power efficiency (left) and the value at 1000 cd m^{-2} (right). (d) The maximum external quantum efficiency (left) and the value at 1000 cd m^{-2} (right). (e) CIE coordinates @EQE$_{max}$.

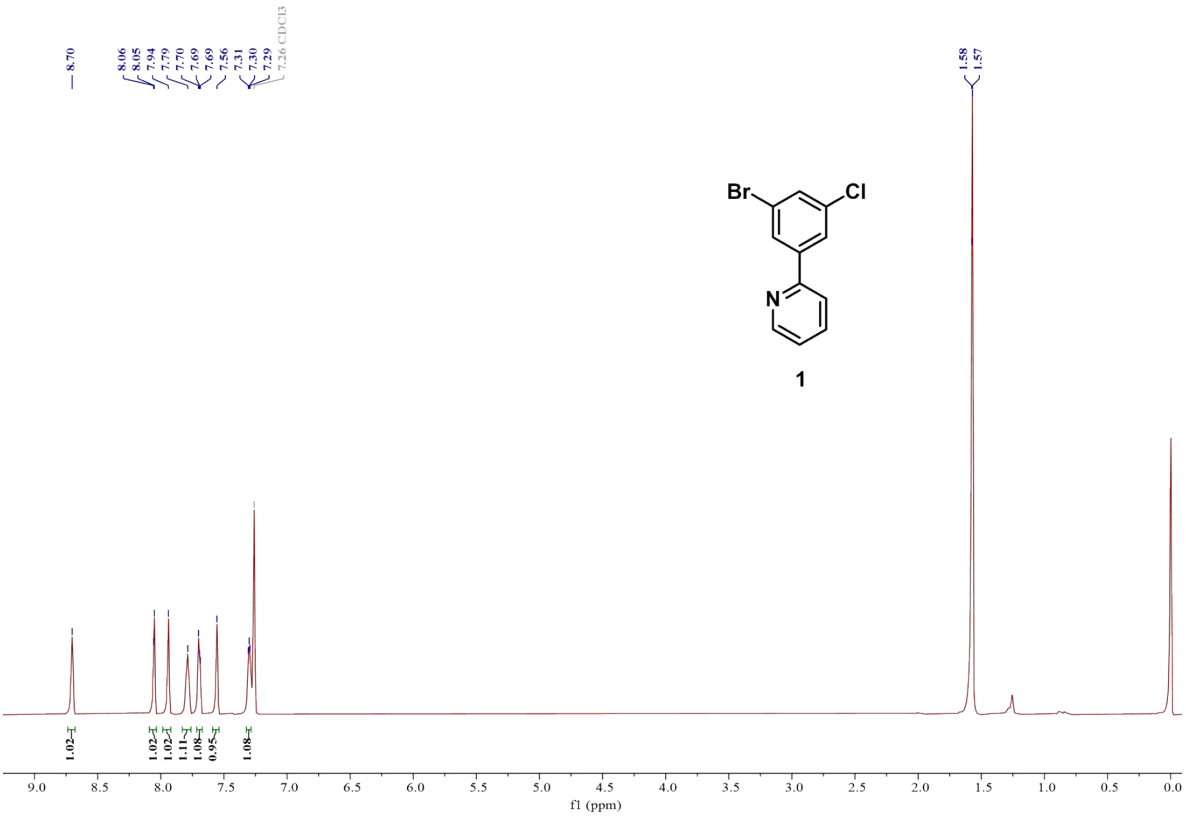

Figure S7. ^{1}H NMR spectrum of **1**.

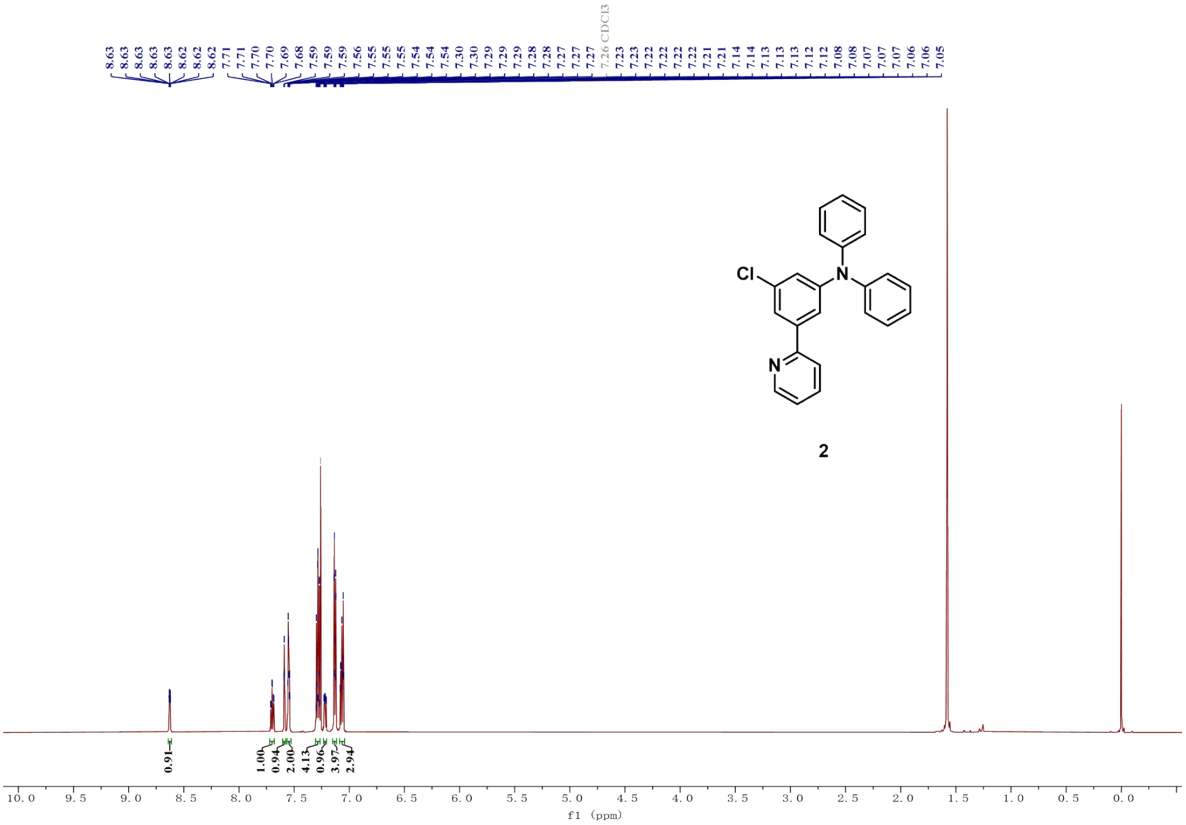

Figure S8. ^{1}H NMR spectrum of **2**.

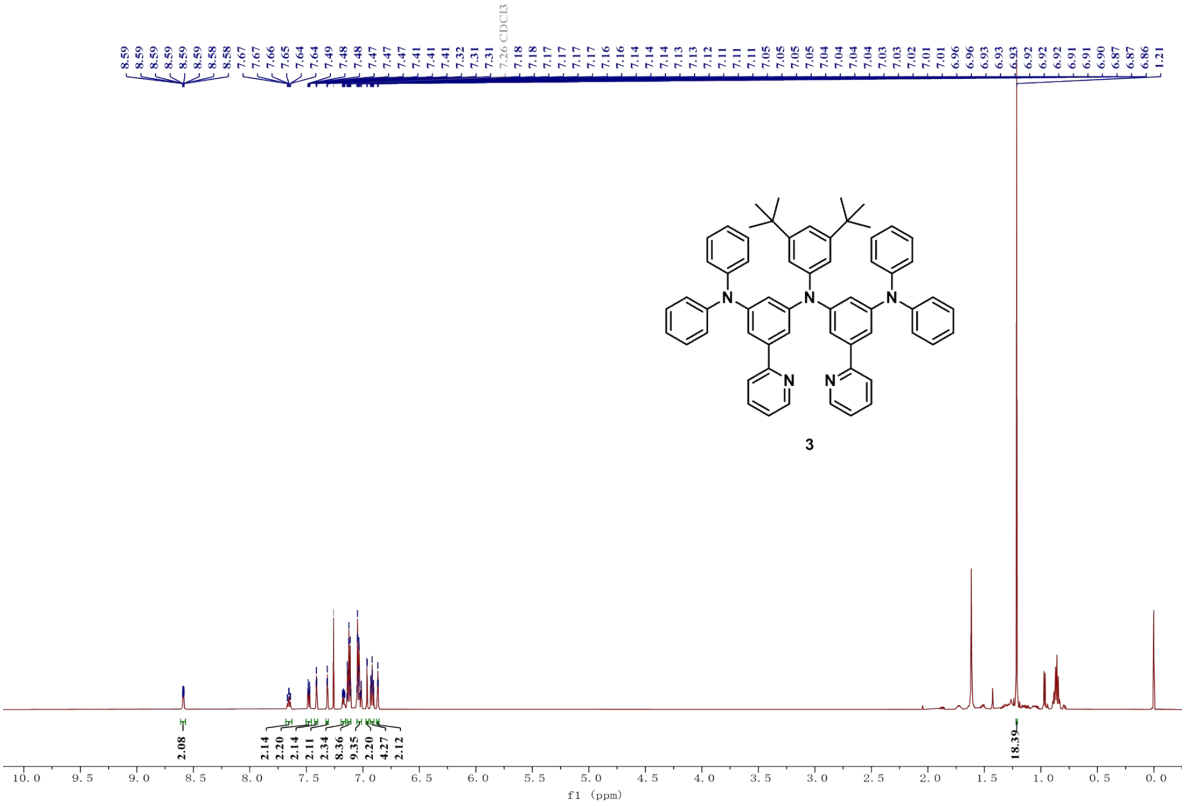

Figure S9. ^{1}H NMR spectrum of **3**.

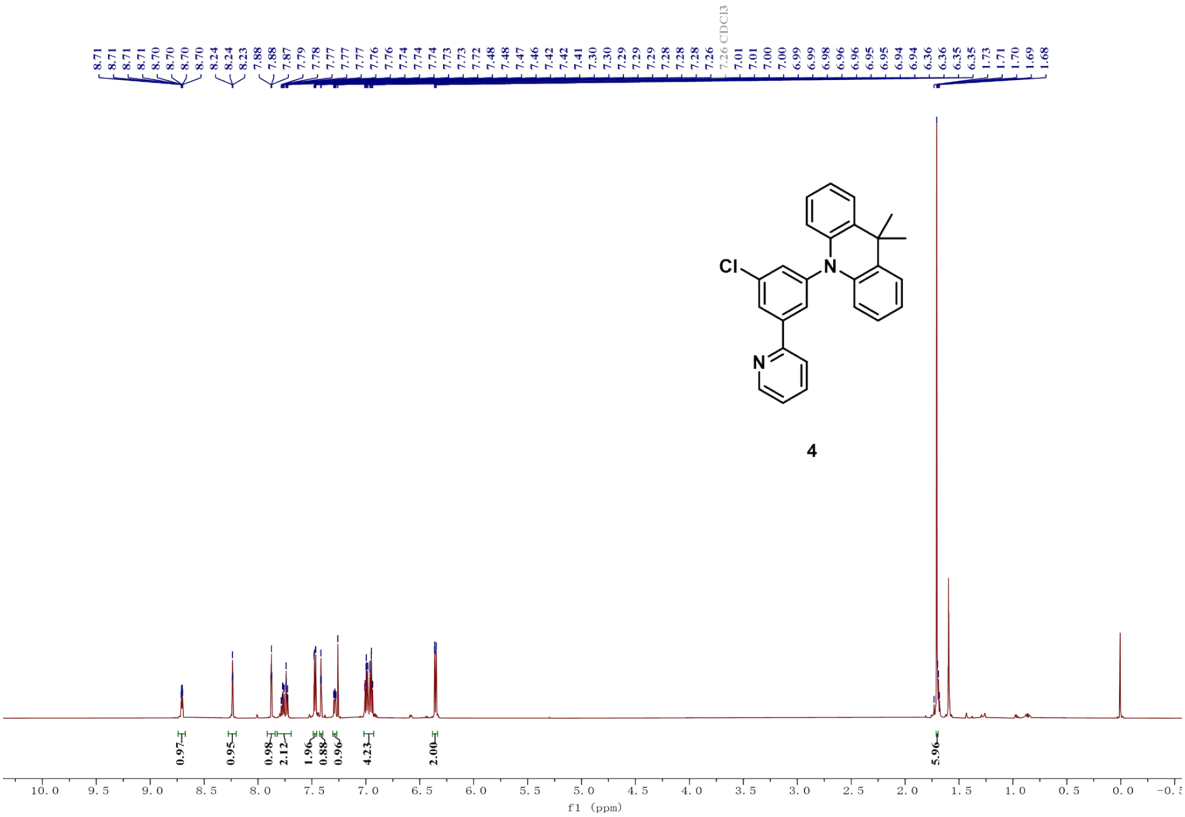

Figure S10. ^{1}H NMR spectrum of **4**.

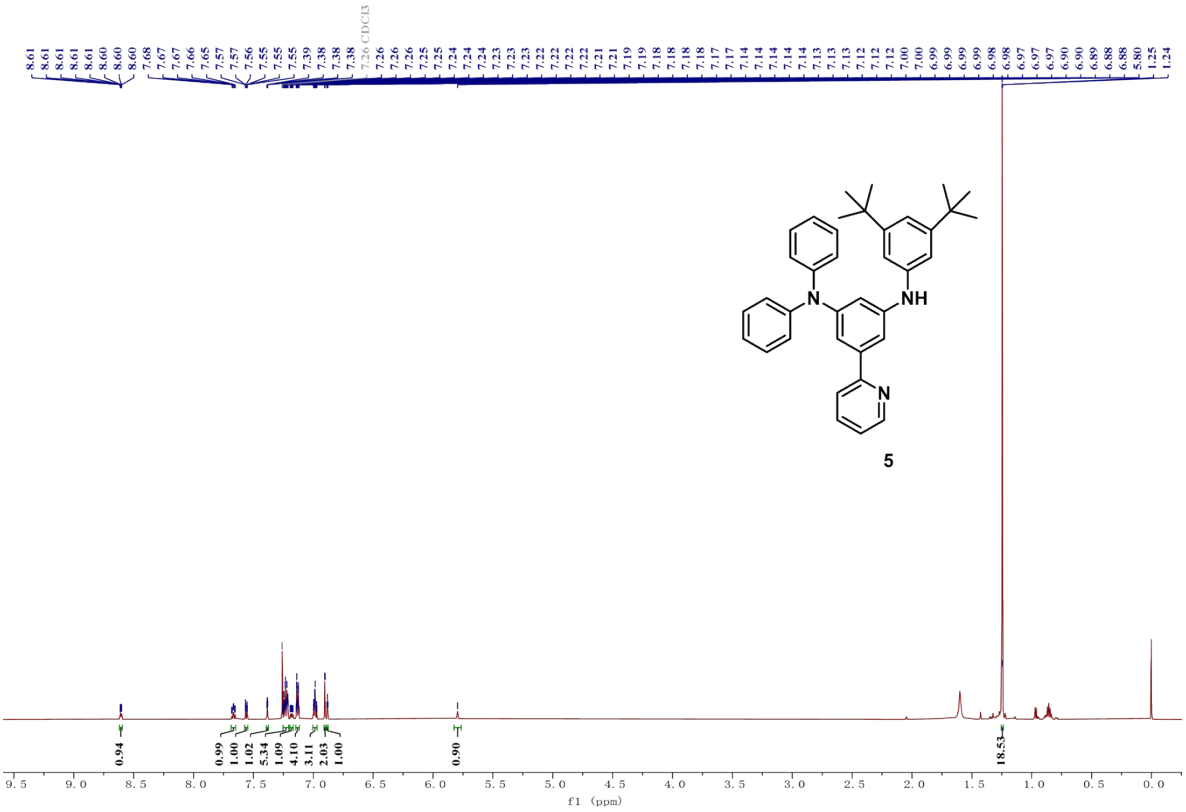

Figure S11. ^{1}H NMR spectrum of **5**.

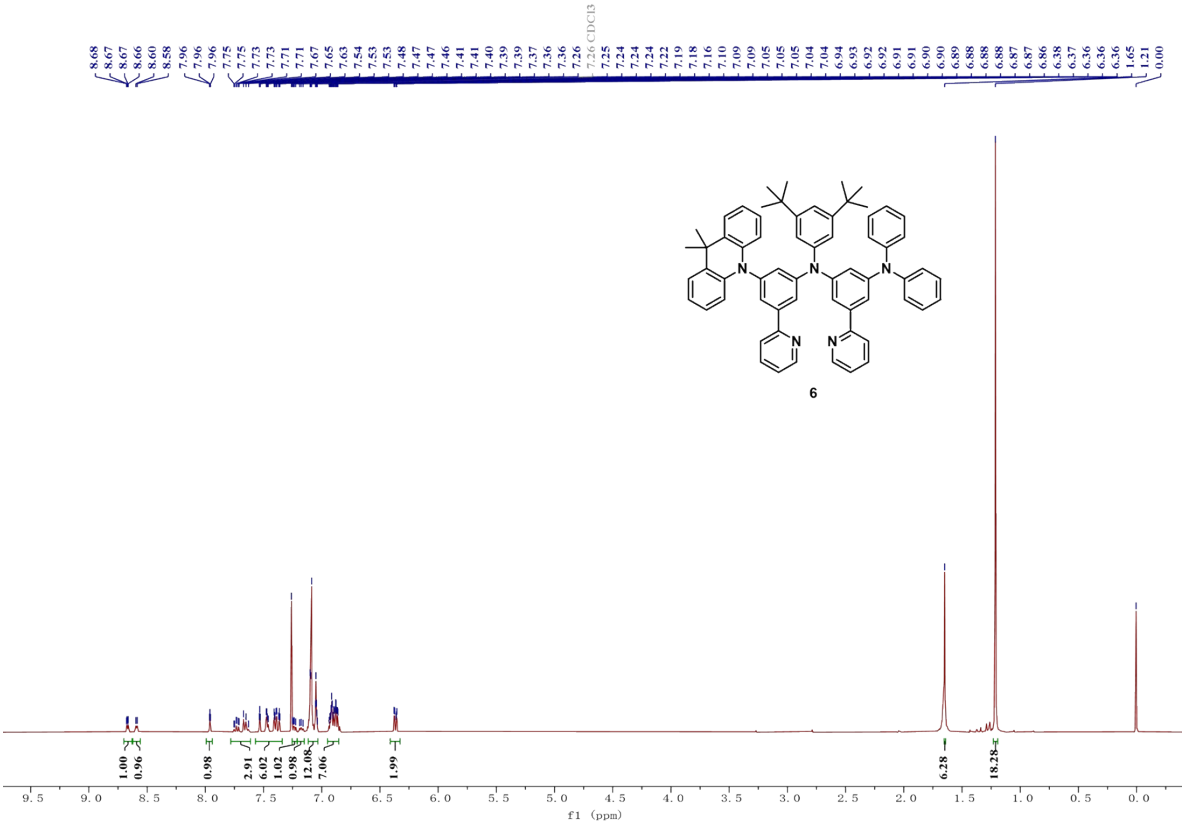

Figure S12. ^{1}H NMR spectrum of **6**.

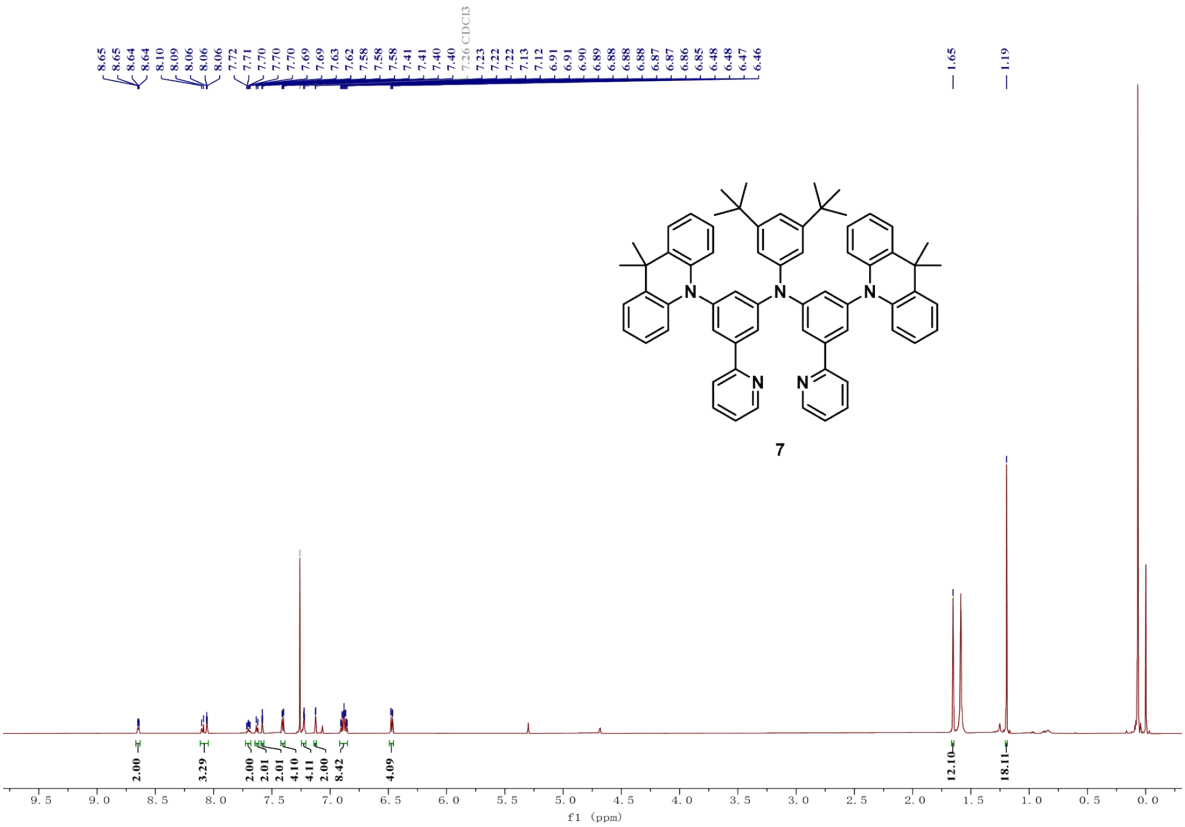

Figure S13. ^{1}H NMR spectrum of **7**.

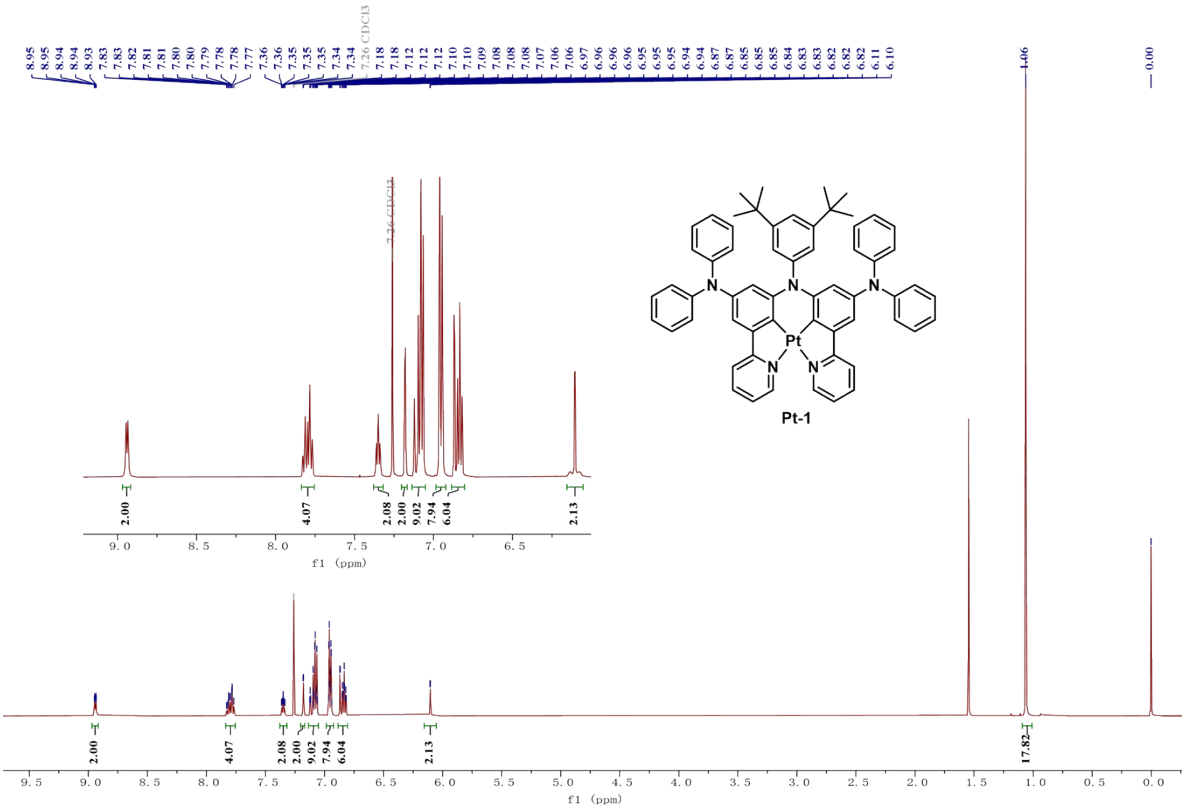

Figure S14. ^{1}H NMR spectrum of **Pt-1**.

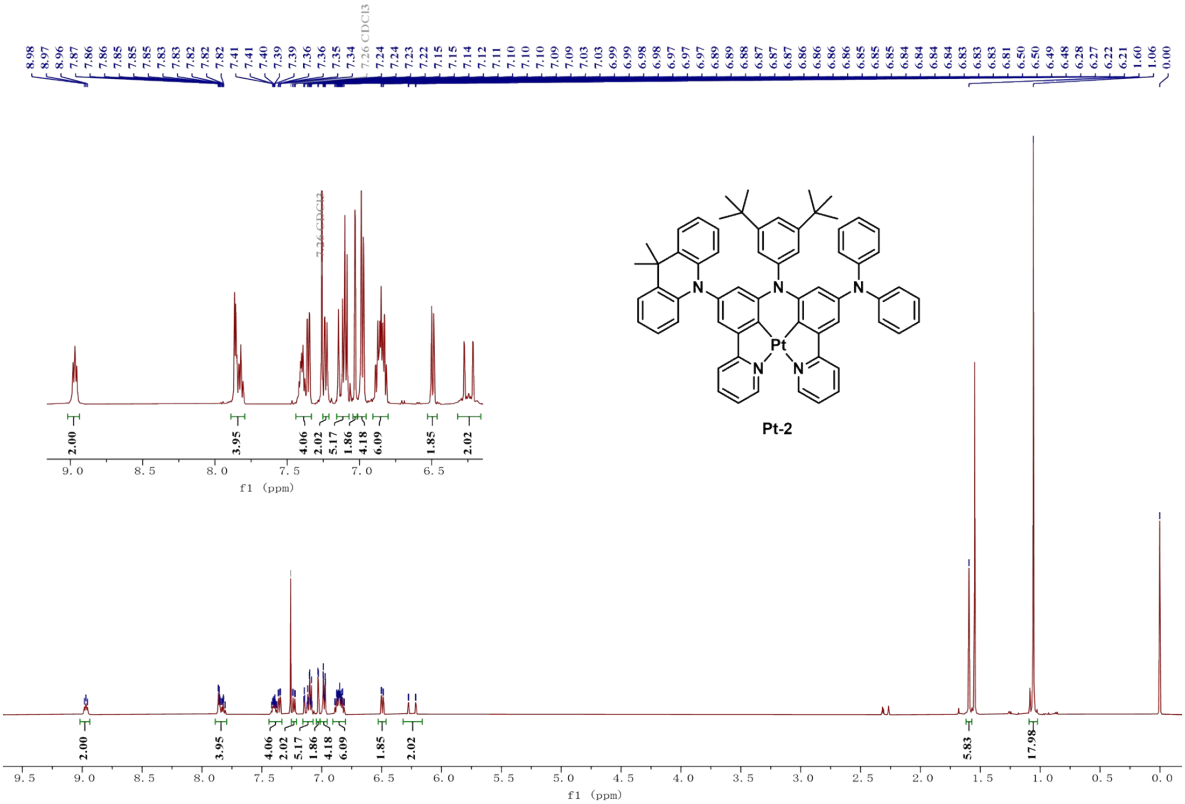

Figure S15. ^{1}H NMR spectrum of **Pt-2**.

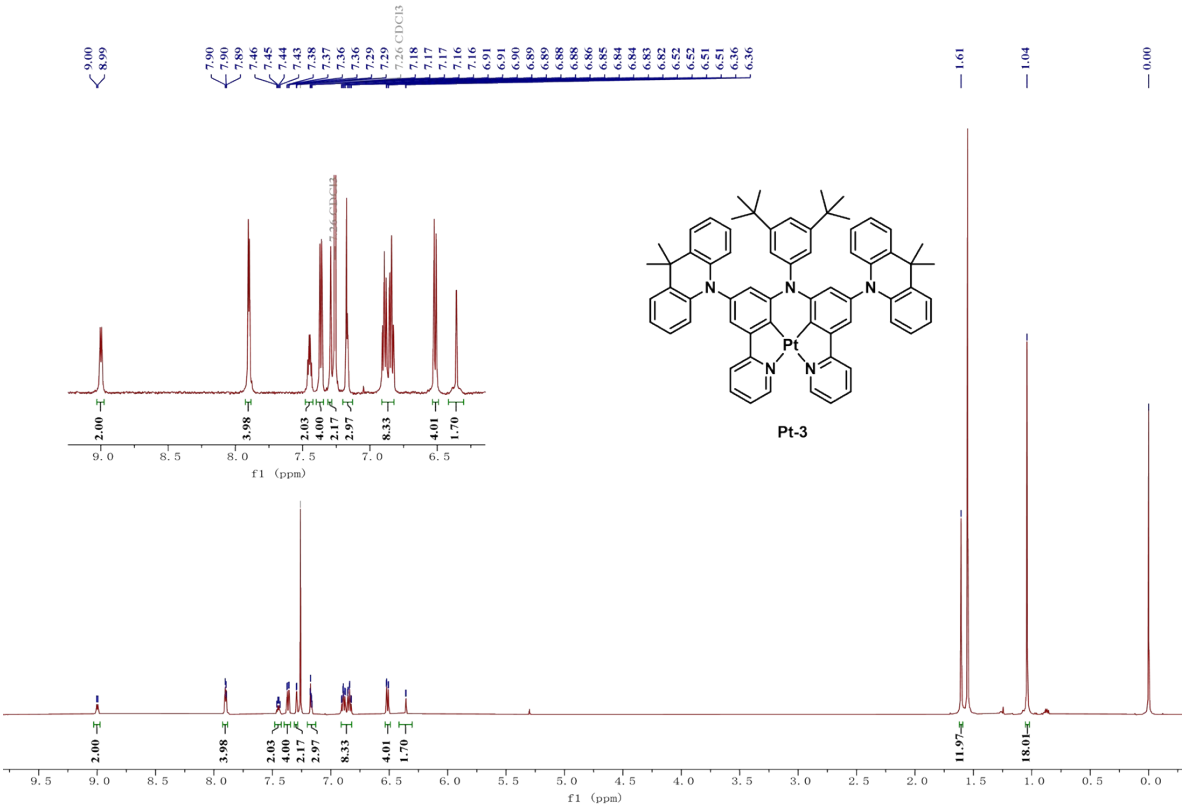

Figure S16. ^{1}H NMR spectrum of **Pt-3**.

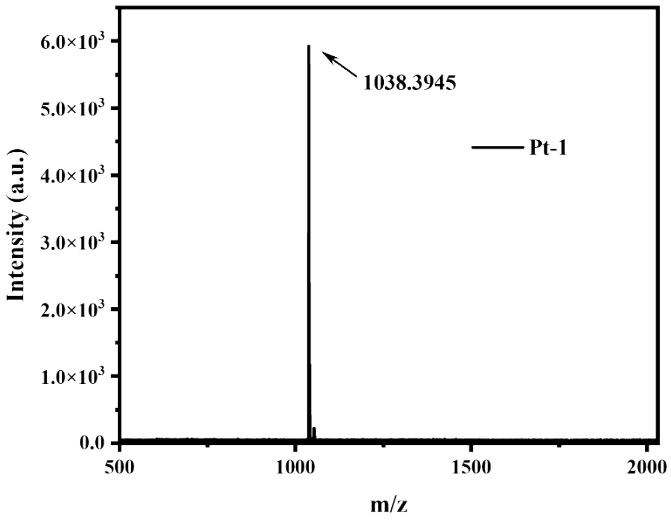

Figure S17. MS spectrum of **Pt-1**.

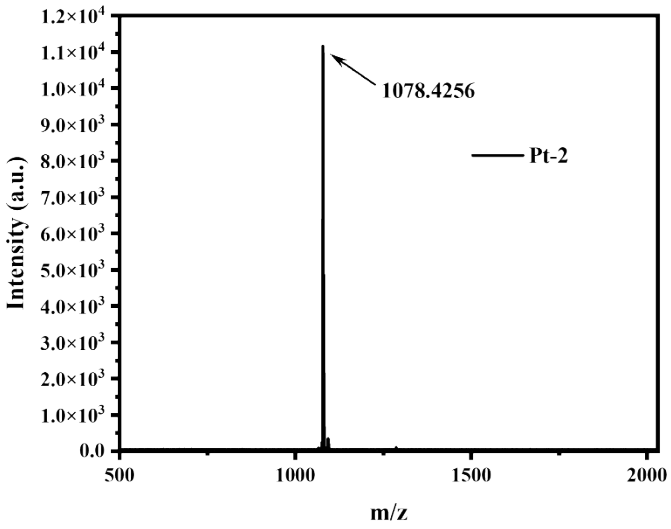

Figure S18. MS spectrum of **Pt-2**.

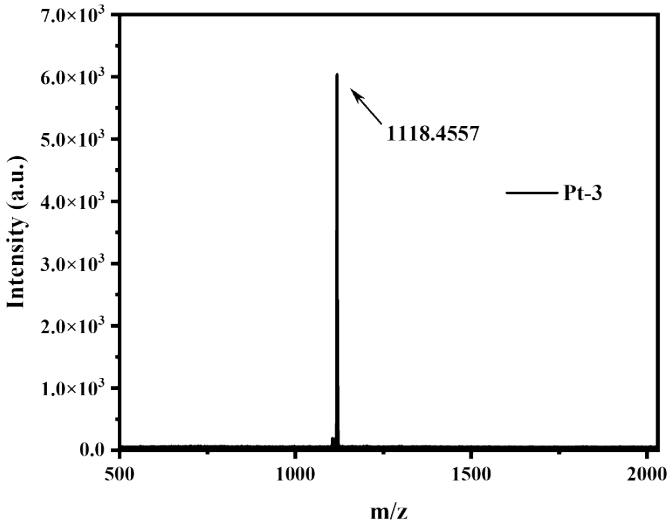

Figure S19. MS spectrum of **Pt-3**.

References

1. V. Dolomanov, L. J. Bourhis, R. J. Gildea, J. A. K. Howard, H. Puschmann, *J. Appl. Cryst.* 2009, **42**, 339-341.

2. G. M. Sheldrick, *Acta. Cryst.* 2015, **A71**, 3-8.

3. G. M. Sheldrick, *Acta. Cryst.* 2015, **C71**, 3-8.

4. M. J. Frisch, G. W. Trucks, H. B. Schlegel, G. E. Scuseria, M. A. Robb, J. R. Cheeseman, G. Scalmani, V. Barone, B. Mennucci, G. A. Petersson, H. Nakatsuji, M. Caricato, X. Li, H. P. Hratchian, A. F. Izmaylov, J. Bloino, G. Zheng, J. L. Sonnenberg, M. Hada, M. Ehara, K. Toyota, R. Fukuda, J. Hasegawa, M. Ishida, T. Nakajima, Y. Honda, O. Kitao, H. Nakai, T. Vreven, J. A. Montgomery Jr, J. E. Peralta, F. Ogliaro, M. Bearpark, J. J. Heyd, E. Brothers, K. N. Kudin, V. N. Staroverov, R. Kobayashi, J. Normand, K. Raghavachari, A. Rendell, J. C. Burant, S. S. Iyengar, J. Tomasi, M. Cossi, N. Rega, J. M. Millam, M. Klene, J. E. Knox, J. B. Cross, V. Bakken, C. Adamo, J. Jaramillo, R. Gomperts, R. E. Stratmann, O. Yazyev, A. J. Austin, R. Cammi, C. Pomelli, J. W. Ochterski, R. L. Martin, K. Morokuma, V. G. Zakrzewski, G. A. Voth, P. Salvador, J. J. Dannenberg, S. Dapprich, A. D. Daniels, Ö . Farkas, J. B. Foresman, J. V. Ortiz, J. Cioslowski, D. J. Fox, Revision D.01 ed., Gaussian, Inc., Wallingford CT, 2009.

5. a) A. D. Becke, J. Chem. Phys. 1993, **98**, 5648; b) P. J. Stephens, F. J. Devlin, C. F. Chabalowski, M. J. Frisch, J. Phys. Chem. 1994, **98**, 11623.

6. P. J. Hay, W. R. Wadt, *J. Chem. Phys*. 1985, **82**, 299.

7. G. A. Petersson, M. A. Al-Laham, *J. Chem. Phys*. 1991, **94**, 6081.